Deep-space glycine formation *via* Strecker-type reactions activated by ice water dust mantles. A computational approach†

Albert Rimola,[a] Mariona Sodupe*[b] and Piero Ugliengo*[a]

Received 9th November 2009, Accepted 17th February 2010
First published as an Advance Article on the web 31st March 2010
DOI: 10.1039/b923439j

A Strecker-type synthesis of glycine by reacting NH_3, $H_2C{=}O$ and HCN in presence of ice water (H_2O–ice) as a catalyst has been theoretically studied at B3LYP/6-31+G(d,p) level within a cluster approach in order to mimic reactions occurring in the interstellar and circumstellar medium (ICM). Results indicate that, despite the exoergonic character of the considered reactions occurring at the H_2O–ice surface, the kinetics are slow due to relatively high electronic energy barriers ($\Delta U_0^{\neq}$ = 15–45 kcal mol^{-1}). Reactions occurring within H_2O–ice cavities, in which ice bulk effects have been modeled by assuming a dielectric continuum (ε = 78), show energy barriers low enough to allow NH_2CH_2OH formation but not $NH{=}CH_2$ ($\Delta U_0^{\neq}$ = 2 and 21 kcal mol^{-1}, respectively) thus hindering the NH_2CH_2CN formation, *i.e.* the precursor of glycine, through Strecker channels. Moreover, hydrolysis of NH_2CH_2CN to give glycine is characterized by high electronic energy barriers ($\Delta U_0^{\neq}$ = 27–34 kcal mol^{-1}) and cannot readily occur at cryogenic temperatures. Nevertheless, the facts that $NH{=}CH_2$ formation can readily be achieved through the radical–radical HCN + 2H → $NH{=}CH_2$ reaction [D. E. Woon, *Astrophys. J.*, 2002, **571**, L177–L180], and that present results indicate that the Strecker step of $NH{=}CH_2$ + HCN → NH_2CH_2CN exhibits a relative low energy barrier ($\Delta U_0^{\neq}$ = 8–9 kcal mol^{-1}), suggest that a combination of these two mechanisms allows for the formation of NH_2CH_2CN in the ICM. These results strengthen the thesis that NH_2CH_2CN could have been formed and protected by icy dust particles, and then delivered through micro-bombardments onto the early Earth, leading to glycine formation upon contact with the primordial ocean.

Introduction

The general fascination with the existence of interstellar and circumstellar molecules of biological interest is mainly due to the direct connection of this subject with chemical evolution and, ultimately, with the origin of life. By means of several spectroscopic observations there is now convincing evidence of the presence of a wide variety of complex organic molecules in the interstellar and circumstellar clouds of gas and dust which pervade the galaxies.[1–6] Space, therefore, might have been an important source of organic molecules for the primordial Earth since some of the terrestrial prebiotic molecules could have firstly been synthesized in the interstellar and circumstellar medium (ICM) and then transported to the early Earth by comets, asteroids and meteorites. However, focusing on the exogenous delivery of extraterrestrial molecules relevant for life (namely, amino acids) one gets involved in a controversy. While careful analyses of carbonaceous chondrite meteorites fallen on Earth[7,8] and, more recently, of dust cometary grains collected by the Stardust spacecraft[9–11] reveal the presence of several amino acids, direct detection of interstellar glycine (the simplest amino acid) is still doubtful.[12–17] Despite that, amino acid precursors (molecules that lead to amino acids, usually after hydrolysis) have indeed been detected, as it is the case of aminoacetonitrile (NH_2CH_2CN), the precursor for glycine formation.[18] Because of that, the search for glycine in ICM is currently the object of intensive work, which requires the development and application of state-of-the-art astronomical instrumentation for spectroscopic observations.

The plausibility of amino acids' formation and their survival under the harsh physical conditions of space have been demonstrated by means of several experiments that simulated the conditions of the interstellar medium in the laboratory: (i) the synthesis of amino acids was successfully accomplished by UV-irradiation of interstellar ice analogs;[19–22] and (ii) amino acids were observed to be photostable only when they were embedded in dust particle analogs.[23] Both experiments highlighted the essential role of the grain particles in the amino acids' synthesis and their survival. This stresses the fact that amino acids cannot be simply formed by gas-phase reactions alone; instead, their formation may be facilitated by the catalytic role played by dust grain ice particles. Other experiments were focused on the thermal reactivity, *i.e.*, without radiation effects, of laboratory interstellar ice analogs composed of H_2O:NH_3:H_2CO at low temperatures (40–100 K).[24,25] Although amino acids formation was not

[a] *Dipartimento di Chimica IFM, NIS Centre of Excellence and INSTM (Materials and Technology National Consortium), UdR torino, Università di Torino, Via P. Giuria 7, 10125 Torino, Italy. E-mail: piero.ugliengo@unito.it*
[b] *Departament de Química, Universitat Autònoma de Barcelona, Bellaterra 08193, Spain. E-mail: mariona@klingon.uab.es*

† Electronic supplementary information (ESI) available: [gas-phase energy profiles and alternative paths]. See DOI: 10.1039/b923439j

detected, it was possible, by means of infrared spectroscopy, to detect the presence of poly-oxymethylene and its derivatives, H_2CO polymers and NH_2CH_2OH as organic residues. Indeed, NH_2CH_2OH is relevant as an intermediate product of the Strecker synthesis, one of the possible routes to synthesize amino acids.

In spite of the experimental evidence, very little is known about the mechanistic steps through which amino acids form. As quoted previously, the oldest and most known postulated mechanism for amino acids formation is the Strecker-type synthesis.[26,27] This reaction has been suggested to occur in ICM and also in the primitive Earth atmosphere, as a possible indigenous amino acid synthesis,[28–30] and is currently the simplest and most economical method for the preparation of α-amino acids in labs at technical scale.[31] The Strecker reaction overall comprises a condensation of an aldehyde or ketone with an amine, the nucleophilic attack of a cyanide molecule, followed by the subsequent hydrolysis of the resulting α-amino nitrile. By means of the simplest reactants, namely formaldehyde $H_2C{=}O$, ammonia NH_3 and hydrogen cyanide HCN, the final product is glycine NH_2CH_2COOH (see Scheme 1). The fact that such reactants are available in relative abundance in ICM, coupled to the fact that UV-photolysis of a H_2O:CH_3OH:NH_3:HCN interstellar ice analog (CH_3OH decomposes to $H_2C{=}O$) resulted in amino acids formation,[19] strengthened the thesis that a Strecker-based reactions may indeed occur in ICM. However, isotopic labeling revealed that the Strecker mechanism accounts only partially for some of the observations,[32] so other mechanisms (*e.g.* radical–radical) or a mixture of them have also been proposed.

Direct experimental measurements to elucidate reaction mechanisms are difficult to perform, whereas, in contrast, quantum mechanical methods can be readily adopted to study a variety of possible reaction mechanisms by exploring the potential energy surfaces (PES). In this context, ion–molecule reactions and radical–molecule mechanisms occurring in the gas-phase have been studied theoretically.[33–40] More recently, the role of ice grain water (H_2O–ice) mantles on the thermal formation of the aminoacetonitrile precursor or glycine has been addressed theoretically[41–47] showing a strong catalytic effect of H_2O–ice, due to the proton mobility at the ice surface itself. This is similar to that observed for heterogeneous reactions occurring on stratospheric ices, which do not proceed in the gas-phase.[48]

In the present work the Strecker reactions occurring at the surface or within a H_2O–ice mantle of a dust grain under the ultracold and high-vacuum conditions present in the ICM have been simulated by quantum mechanical methods based on density functional theory. For the first time, the whole Strecker mechanism (*i.e.* the condensation of $H_2C{=}O$, NH_3 and HCN to form glycine) on a cluster model mimicking

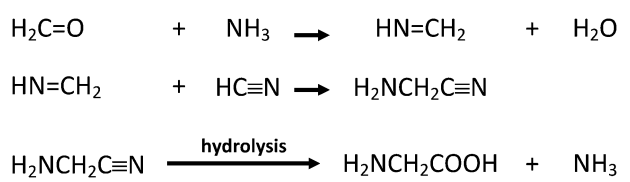

Scheme 1

crystalline H_2O–ice has been addressed, with the aim that the present results will contribute to understanding the ease with which the reactive channels yield glycine precursors.

Computational details

All calculations have been performed using the GAUSSIAN03 package program.[49] The structure of each stationary point has been fully optimized using the hybrid B3LYP[50,51] functional with the 6-31 + G(d,p) basis set. All structures have been characterized by the analytical calculation of the harmonic frequencies as minima (reactants, intermediates and products) and saddle points (transition states). For more difficult cases, we have carried out intrinsic reaction coordinate (IRC) calculations at the same level of theory to ensure that a given transition structure connects the expected reactants and products. The zero point energy (ZPE)-corrected and Gibbs free energy profiles were obtained by computing the thermochemical corrections to the energy values using the standard harmonic oscillator formulae computed at B3LYP/6-31 + G(d,p).[52] In order to account for long-range effects of the H_2O–ice bulk matrix on the energy profiles, single-point energy calculations using the conductor polarized continuum model (CPCM)[53,54] have been carried out at the optimized gas-phase geometries considering the dielectric constant of ice as equal to that of water (see discussion below). The ZPE-corrected energy profiles including bulk effects were estimated by including the gas-phase ZPE corrections on the CPCM-electronic energies.

Results and discussion

Ice model

According to a cyclic evolutionary model of interstellar dusts,[55] in molecular clouds, dust grains consist of a core composed of refractory materials such as silicate and amorphous carbon particles, and of a mantle of different frozen molecules covering the core, where ice water is generally the most abundant constituent. At the extremely low pressures and temperatures at which icy grain mantles form, the dominant morphology is probably a high-density amorphous ice.[56–58] In contrast, when the ice is warmed up, H_2O molecules re-arrange in a crystalline structure, so that both amorphous and crystalline phases are present in ICM. Crystalline ices have indeed been detected in ICM and in cometary comas,[59–63] and laboratory experiments suggest that their formation may be due to the exposition of dust particles to temperatures of about 150–200 K.[64,65]

Modelling at an *ab initio* level an amorphous material is rather problematic because its disordered nature implies the presence of various surface sites and defects so that, one needs to adopt large unit cells, rendering the calculations very demanding. Nonetheless, for the particular case of ice water, a combined experimental and theoretical work of Allouche *et al.*[66] intended to analyze the adsorption of CO on different amorphous and nanocrystalline ice samples concluded that, at the molecular scale, the amorphous ice can be partly considered as an ordered material. Based on these results, in the present

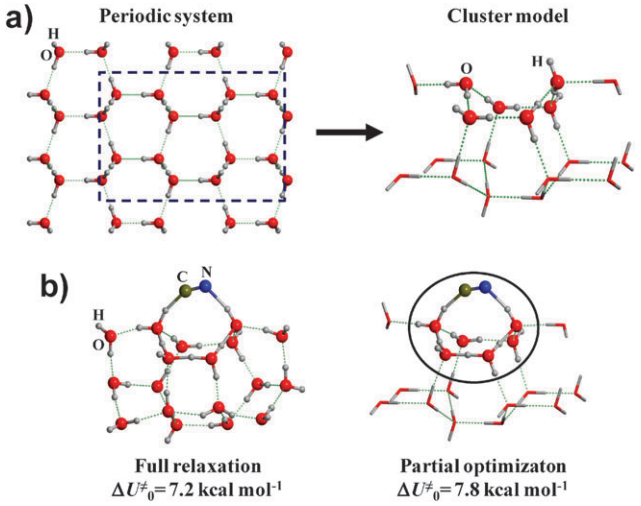

Fig. 1 (a) Periodic system and cluster model H_2O–ice of the proton-ordered crystalline Ice XI. The cluster model derives from the (010) ice surface. (b) Transition state structures of the CNH → HCN isomerization occurring on the cluster model of Ice XI. The left-most structure results from a full geometry relxation of the cluster; the right-most structure results from a partial optimization, which includes the atoms inside the circle. ZPE-corrected energy barriers (kcal mol^{-1}) computed at B3LYP/6-31 + G(d,p) level are also included.

work, we have resorted to a given crystalline ice phase to model the H_2O–ice mantle. On Earth, the naturally occurring stable form of ice at low pressures and temperatures is hexagonal ice, Ih. Ih is a proton-disordered system, and because the position of the protons follows the Bernal–Fowler–Pauling (BFP) rules[67,68] a structural model for Ih envisaging all the hypothetical proton-ordered substructures in agreement with the BFP rules would be very costly to treat quantum mechanically. Ice XI is a proton-ordered low-temperature analogue of ice Ih, which is formed in the presence of a minute amount of hydroxide anions at 72 K[69] and is the one that has been adopted here as the crystalline model (see Fig. 1a, periodic system). The theoretical study of both bulk and surface structures of ice XI allows to adopt it as a reasonable model for a disordered ice water, because it reflects properly its physico-chemical features in a cost-effective way.[70–73]

In the present work, we have adopted the cluster model that arises from the (010) ice XI surface, shown in Fig. 1a (cluster model). This H_2O–ice model shows two relevant features that need some consideration. First, the cluster becomes dramatically deformed upon full geometry optimization due to the formation of extra hydrogen bonds (H-bonds) at the edge of the cluster, not present in the bulk structure. Thus, in order to overcome such artifact, the atomic positions where the reactions are expected to occur (atoms depicted as balls in Fig. 1a) have been fully optimized, while keeping the atoms at the frontier (atoms depicted as cylinders in Fig. 1a) fixed at their crystal positions. This strategy, while limiting the deformation of the cluster may result in a general increase of the energy barriers for the considered reactions. Second, the icy cluster surface structure allows for an easier proton-transfer between icy protons and the adsorbed molecules by what is called the "proton relay" mechanism. Theoretical works evidenced a strong catalytic effect of this mechanism,[74,75] including astrochemical reactions occurring at H_2O–ice surfaces.[41,43]

Some calibration of the H_2O–ice cluster model was carried out to compute the energy penalty due to the geometrical constraints and to check for the catalytic effect on a possible proton assisted mechanism. The CNH/HCN isomerization in presence of the H_2O–ice model was chosen as a model reaction by performing both full and partial geometry relaxation of the cluster. Results are shown in Fig. 1b and reveal that: (i) the ZPE-corrected energy barriers ($\Delta U^{\neq}_0$) for the full and the partial relaxation cases are in excellent agreement with each other (7 and 8 kcal mol^{-1}, respectively); and (ii) the H_2O–ice cluster does catalyse the reaction compared to gas-phase ($\Delta U^{\neq}_0$ = 30 kcal mol^{-1}, see Fig. S1 in the ESI†) by helping the H-exchange *via* surface proton relay scheme. In view of these results, the constrained crystalline-based H_2O–ice cluster was adopted as a model catalyst for the formation of glycine *via* Strecker reactions.

Strecker reaction on H_2O–ice

As mentioned, the Strecker synthesis consists of several chemical reactions to form α-amino acids. The proposed mechanism is sketched in Scheme 1, which focuses on glycine formation. The reaction starts by water elimination between ammonia and formaldehyde to give methanimine NH=CH_2 as an intermediate. Subsequently, the carbon atom of HCN bonds the carbon atom of NH=CH_2 to give aminoacetonitrile NH_2CH_2CN as the α-aminonitrile intermediate. Finally, hydrolysis of NH_2CH_2CN leads to the formation of glycine as the final α-amino acid product.

The isolated gas-phase reactions of the Strecker mechanism were computed at the B3LYP/6-31 + G(d,p) level of theory, resulting in energy barriers with $\Delta U^{\neq}_0$ in the 40–55 kcal mol^{-1} range (ZPE-corrected energy profiles and optimized structures reported in Fig. S2, S3 and S4 of the ESI†), so that reactions would barely occur under these conditions.

In the following, each step of the Strecker mechanism is studied in the presence of the H_2O–ice cluster model to assess its catalytic role. For all calculations we have assumed that the reactants are in close proximity to each other when contacted with the ice water. Rigorously, diffusion of the species on the surfaces or in the ice bulk is completely negligible, except for H atoms, if no energy inputs exist. Nevertheless, the harsh physical conditions of space ensure the action of several energy inputs such as UV radiation, cosmic rays, and shock waves onto the ice mixtures, so that, at least in principle, diffusion of the reactants to come closer is expected to easily occur. Despite that, however, it is worth mentioning that UV effects, assumed to be essential in laboratory experiments, have not been taken into account in the present work; that is, only neutral closed-shell species have been considered in the reactions. There are two reasons for that: (i) dealing with open-shell systems would dramatically increase the complexity of the problem and the computational burden; and (ii) the scope of the work is to determine the intrinsic role (namely, without external agents) of the H_2O–ice mantles in the interstellar and circumstellar processes as well as to estimate the most

favorable reactive channels of the Strecker synthesis at cryogenic temperatures. The role of UV radiation and cosmic rays will be addressed in future work.

Methanimine $NH{=}CH_2$ formation. Ammonia adds to formaldehyde by a concerted nucleophilic attack of the N atom towards the carbonyl C atom and a proton transfer from NH_3 to the carbonyl O to give the NH_2CH_2OH intermediate, which is then converted to $NH{=}CH_2$ by water elimination. The catalytic role played by the H_2O–ice cluster is seen in the computed ZPE-corrected energy profile shown as Step 1 of Fig. 2. Starting from the pre-reactant complex **R1**, the condensation between NH_3 and $H_2C{=}O$ occurs through a transition state $\mathbf{TS1_1}$ with the development of a direct N–C bond and the proton transfer from NH_3 to $H_2C{=}O$ as favoured by the proton relay mechanism within the H_2O–ice cluster. For this process the computed $\Delta U_0^{\neq}$ is 9.6 kcal mol^{-1}, with the intermediate NH_2CH_2OH ($\mathbf{I1_1}$) being 7.1 kcal mol^{-1} lower in energy than **R1**. $\mathbf{I1_1}$ is a H-bond complex between NH_2CH_2OH and H_2O–ice cluster, whose configuration is not suitable for the successive water elimination. Nevertheless, rotation by 180° of NH_2CH_2OH as a whole (costing around the interaction energy, *i.e.* 9 kcal mol^{-1}), gives $\mathbf{I1_2}$ (0.3 kcal mol^{-1} above $\mathbf{I1_1}$) from which the release of water through $\mathbf{TS1_2}$ (14.5 kcal mol^{-1} with respect to **R1**) leads to $NH{=}CH_2$ with a final ZPE-reaction energy ($\Delta_r U_0$) of −6.2 kcal mol^{-1}. The $\Delta U_0^{\neq}$ values for the analogue reactions in gas-phase are 32 kcal mol^{-1} and 44 kcal mol^{-1} for the first and second process, respectively, while the final $\Delta_r U_0$ is −1 kcal mol^{-1} (see the ESI for gas-phase reactions†). These data show that the H_2O–ice mantle does indeed lower the considered reactions compared to those occurring in gas-phase.

The reaction of H_2 with HCN also leads to the formation of $NH{=}CH_2$. This reaction has also been studied due to the abundance of H_2, although it is not involved in the Strecker mechanism. The computed gas-phase calculations gives $\Delta U_0^{\neq}$ = 85 kcal mol^{-1} and $\Delta_r U_0$ = −10 kcal mol^{-1}, which become 49 kcal mol^{-1} and −13 kcal mol^{-1}, respectively, when it occurs at the surface of the crystalline H_2O–ice (data available in Fig. S5 of the ESI†).

Aminoacetonitrile NH_2CH_2CN formation. The gas-phase reaction bewteen HCN and $NH{=}CH_2$ does not yield $NH_2CH_2\mathbf{CN}$, but its isomer $NH_2CH_2\mathbf{NC}$ (17 kcal mol^{-1} less stable). This has been computed already by Koch *et al.*[43] and is confirmed by the present calculations (see the ESI† for details). Thus, in the gas-phase, two steps are needed to form aminoacetonitrile: (i) promotion of HCN into its isomer CNH; and (ii) reaction of CNH with $NH{=}CH_2$. This process is energetically costly since $\Delta U_0^{\neq}$ values for the isomerization and for the aminoacetonitrile formation are 44 and 40 kcal mol^{-1}, respectively (see Fig. S3 of the ESI† for details). Fortunately, the HCN/CNH isomerization is catalyzed by the presence of the H_2O–ice mantle (see Fig. 1b). Indeed, calculations in the presence of crystalline H_2O–ice model (Fig. 3a, Step 2-*i*) shows that the isomerization of HCN from **R2-*i*** results in a $\Delta U_0^{\neq}$ of 18.0 kcal mol^{-1} ($\mathbf{TS2_1}$-***i***), and the resulting H-bonded intermediate ($\mathbf{I2_1}$-***i***) is 10.3 kcal mol^{-1} higher in energy than **R2-*i***. As shown by Fig. 3a, the above process occurs in presence of $NH{=}CH_2$, which remains physisorbed to H_2O–ice as an inert species. H-bond rearrangement in $\mathbf{I2_1}$-***i*** leads to the nearly degenerate $\mathbf{I2_2}$-***i*** intermediate, which can evolve to aminoacetonitrile **P2-*i*** through a $\Delta U_0^{\neq}$ of 29.9 kcal mol^{-1} ($\mathbf{TS2_1}$-***i*** with respect to the **R2-*i*** reference state). These data show that the final product **P2-*i*** is thermodynamically very favorable (−15.2 kcal mol^{-1}) and that the H_2O–ice exerts a noticeable catalytic effect. The same reaction was computed by Koch *et al.*, obtaining an energy barrier of 22 kcal mol^{-1}. The energy differences can be rationalized by considering that Koch *et al.* used three completely free water molecules to simulate the amorphous icy particle, resulting in more degrees of freedom to stabilize the activated complex. Nevertheless, for both

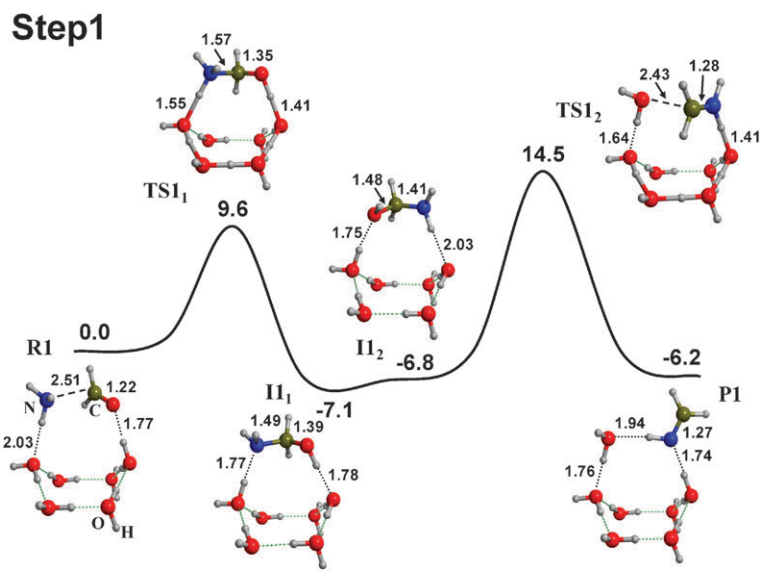

Fig. 2 ZPE-corrected B3LYP/6-31+G(d,p) potential energy profile for the reaction $NH_3 + H_2C{=}O \rightarrow NH{=}CH_2 + H_2O$ (Step 1) in presence of H_2O–ice model following the Strecker mechanism. Relative energy values refer to the **R1** structure. Energies in kcal mol^{-1}; bond distances in Å. Only the optimized part of the H_2O–ice model is shown for the sake of clarity.

cases, the computed energy barriers are rather high for the ICM conditions, so that alternative reaction paths may be feasible.

One of the main features of water, irrespective of its state, is its capacity to stabilize charged species. In the ICM this is not an exception and, indeed, it is widely accepted that both anions and cations exist in space, probably confined within ice water, as theoretical results pointed out.[76] Following this idea, Koch *et al.* reported a new mechanism for the amino-acetonitrile formation arising from the reaction between CN^- and $NH_2{=}CH_2^+$, in which both ionic species are stabilized by water molecules.[43] In the gas-phase this process cannot proceed because of the extremely high energy barrier due to charge separation cost. However, icy particles may screen charged species, so that this mechanism is analyzed in presence of the crystalline H_2O–ice model. Results are shown in Fig. 3b (Step 2-*ii*). The first barrier refers to the formation of the CN^- and $NH_2{=}CH_2^+$ ions, in which the proton of HCN is transferred to the nitrogen atom of $NH{=}CH_2$ *via* a proton relay mechanism involving two H_2O molecules of the six-membered ring of H_2O–ice. The $\Delta U_0^{\neq}$ for this transfer is 17.5 kcal mol^{-1} (**TS2$_1$-*ii***) and the resulting intermediate **I2-*ii***, which carries the $(CN^-)/(NH_2{=}CH_2^+)$ ion pair, remains 15.5 kcal mol^{-1} above **R2-*ii***. From **I2-*ii***, the C–C bond formation leads to NH_2CH_2**CN** with a $\Delta U_0^{\neq}$ = 16.2 kcal mol^{-1} (**TS2$_2$-*ii***) with respect to **R2-*ii*** and a negative $\Delta_r U_0$ of −14 kcal mol^{-1} (**P2-*ii***). It is worth to note that, if **I2-*ii*** is taken as the reference state for the $(CN^-)/(NH_2{=}CH_2^+)$ reaction, the process for the aminoacetonitrile formation is practically barrierless. This observation highlights the role of polar ices as plausible drivers to induce astrochemical ion pair reactions at low energy cost. It is worth mentioning that if a C–N bond formation from **I2-ii**

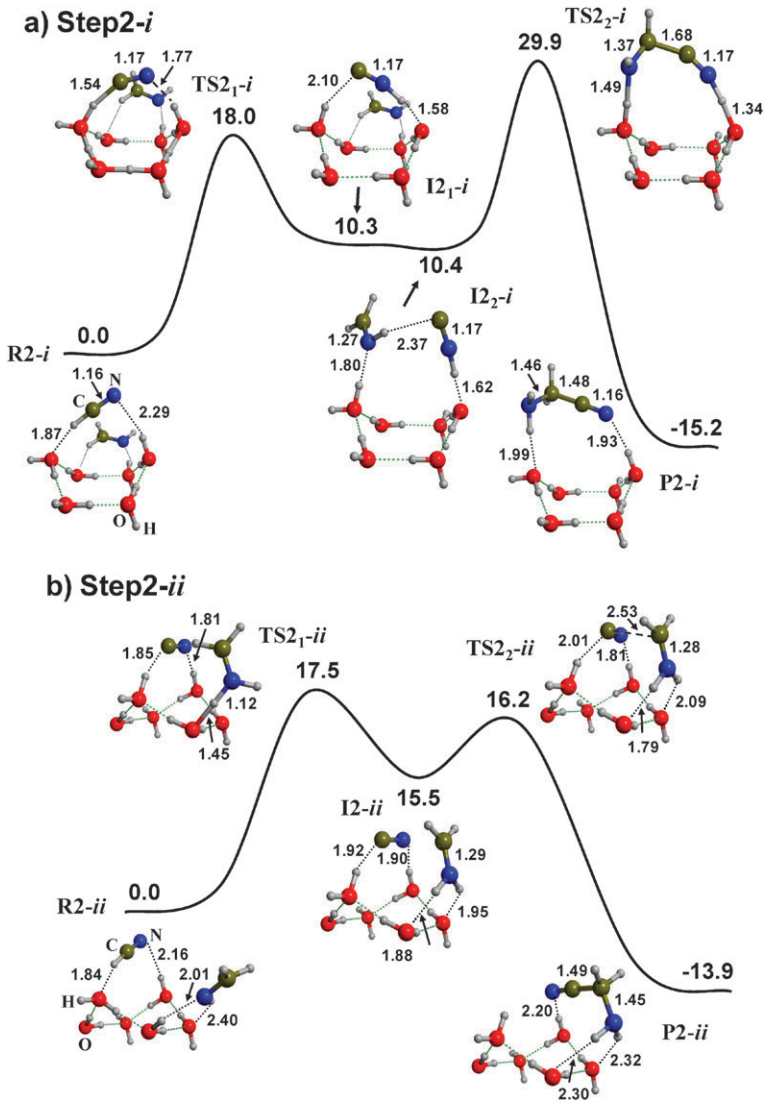

Fig. 3 ZPE-corrected B3LYP/6-31 + G(d,p) potential energy profile for the reaction of HCN + $NH{=}CH_2$ → NH_2CH_2CN in presence of H_2O–ice model following the Strecker mechanism. Two different reactive channels are shown: (a) Step 2-*i*, involves the HCN →CNH isomerisation followed by condensation with $NH{=}CH_2$; (b) Step 2-*ii*, involves the formation of a $(CN^-)/(NH_2{=}CH_2^+)$ ion pair followed by the reaction of the two ions. Relative energy values refer to R2-*i* and R2-*ii* structures for Step 2-*i* and Step 2-*ii*, respectively. Energies in kcal mol^{-1}; bond distances in Å. Only the optimized part of the H_2O–ice model is shown for the sake of clarity.

occurs, the final product would be the NH_2CH_2**NC** isomer. Although the energy barrier is similar to the other path, the $\Delta_r U_0$ is positive so its formation is thermodynamically unfavoured (see Fig. S6 of the ESI† for details).

Hydrolysis of NH_2CH_2CN. The final steps leading to glycine formation envisage the nucleophilic attack of one H_2O molecule towards the nitrile group of NH_2CH_2CN to give $NH_2CH_2C(=O)NH_2$ (Fig. 4a, Step 3), followed by the nucleophilic attack of a second H_2O molecule to the carbonyl C atom to give ammonia and glycine $NH_2CH_2C(=O)OH$ as final products (Fig. 4b, Step 4). In liquid water, the hydrolysis of NH_2CH_2CN towards glycine is immediate; clearly this will not be the case on icy particles in which water mobility is reduced by the crystalline field and by the very low temperatures. Here, the H_2O molecules responsible of steps 3 and 4 are assumed to derive from evaporation processes occurring at the icy surface particles so that in the calculation they have been added to the reaction as they were coming from gas-phase.

Results for the first and second H_2O additions are reported in Fig. 4, Step 3 and Step 4, respectively. The first H_2O nucleophilic attack (Fig. 4a) involves the $C_{nitrile}$–O_{water} bond formation along with a proton transfer (assisted by the H_2O–ice) from water to the $N_{nitrile}$ atom. This process exhibits a large $\Delta U_0^{\neq}$ of 37.9 kcal mol^{-1} (**TS3$_1$**) and the resulting $NH_2CH_2C(-OH)NH$ intermediate **I3** corresponds to the enol tautomeric form of 2-aminoacetamide. The keto-enol tautomerization given through a proton relay ring transition state (**TS3$_2$**) of low activation energy ($\Delta U_0^{\neq}$ = 4.8 kcal mol^{-1} with respect to **R3**) leads to the more stable keto $NH_2CH_2C(=O)NH_2$ form (**P3**). The second H_2O nucleophilic attack proceeds similarly to the first one (Fig. 4b); *i.e.*, C_{amide}–O_{water} bond is formed simultaneously to a proton transfer from water to the N_{amide} atom, followed by ammonia elimination. However, at variance with the previous steps, this one proceeds without a direct proton assistance from the H_2O–ice cluster (see **TS4**) with a $\Delta U_0^{\neq}$ value of 39.0 kcal mol^{-1}. The same process directly assisted by the H_2O–ice cluster has

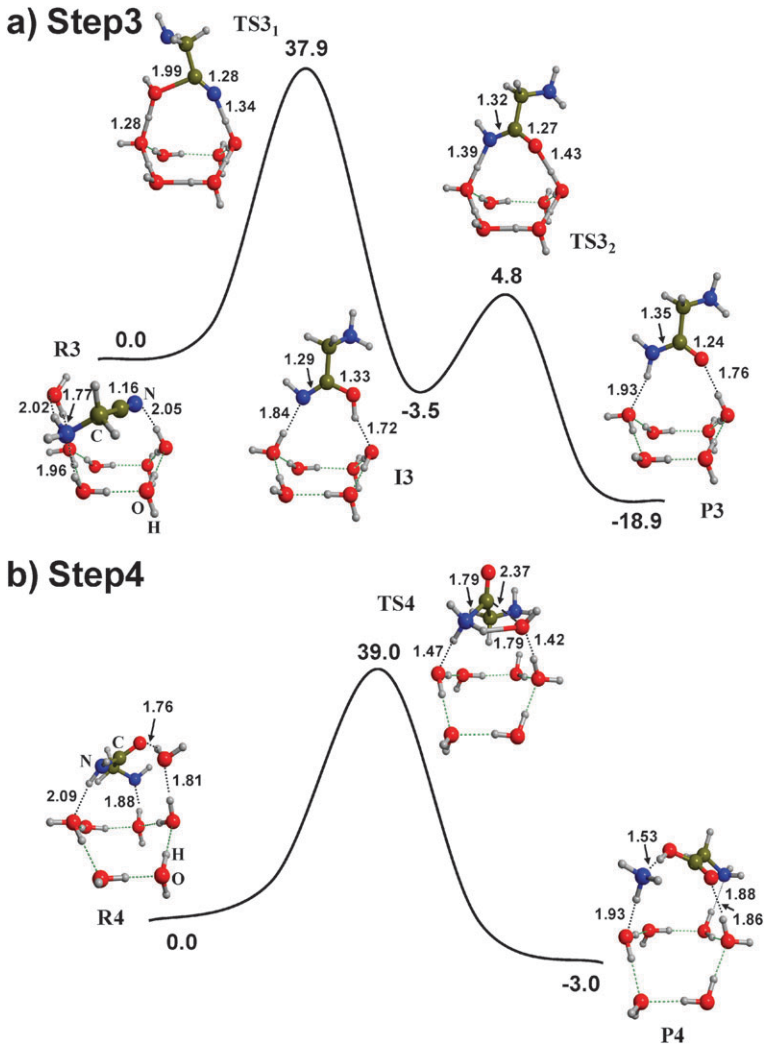

Fig. 4 ZPE-corrected B3LYP/6-31 + G(d,p) potential energy profile for reaction (a) $NH_2CH_2CN + H_2O \rightarrow NH_2CH_2C(=O)NH_2$ (Step 3) and (b) $NH_2CH_2C(=O)NH_2 + H_2O \rightarrow NH_2CH_2C(=O)OH + NH_3$ (Step 4) in presence of H_2O–ice model following the Strecker mechanism. Relative energy values refer to **R3** and **R4** structures for Step 3 and Step 4, respectively. Energies in kcal mol^{-1}; bond distances in Å. Only the optimized part of the H_2O–ice model is shown for the sake of clarity.

also been studied (see Fig. S7 of the ESI† for details): the computed $\Delta U_0^{\neq} = 50.8$ kcal mol^{-1} is, however, much higher than the case in which the water molecule remained far from the icy particle. The reason for the higher barrier of the latter process can be explained by considering that the highest energy **TS4** (see Fig. S7, the ESI†) envisages the icy particle as proton donor towards the NH_2 group and as proton acceptor from the water involved in the nucleophylic attack. This implies a large and costly proton rearrangment within the icy surface ring, which is absent for the **TS4** of Step 4 (Fig. 4), in which the icy particle more naturally acts as proton acceptor from the NH_3^+ group and as proton donor to the OH^- moiety.

Environmental factors affecting reaction profiles

Most of the considered energy profiles exhibit rather high energy barriers for these reactions to easily occur within the ICM physico-chemical conditions. However, the computed profiles are based on ZPE-corrected values, that is, $T = 0$ K and the cluster is considered isolated from its surroundings. In order to have a deeper insight onto the possible role of different environmental factors, the effect of temperatures higher than 0 K and the co-presence of H_2O–ice bulk surrounding the active surface have been investigated on Step 1, Step 2-*ii*, Step 3 and Step 4, respectively.

Temperature effects. Deep-space is usually at ultra-cold temperatures, namely between 10–20 K. However, particular regions can have higher temperatures, as is the case of hot molecular cores, whose temperature may range between 100–200 K. Due to that, the thermochemistry of the stationary points involved in the different reactions paths has been computed at $T = 10$, 100 and 200 K. The new relative free energy values computed at these temperatures (ΔG_T) are reported in Table 1. It is worth noting that at $T = 200$ K water in the ICM is totally desorbed, so that ΔG_{200} values have been provided just to emphasize the trend with increasing T. In most of the stationary points the relative ZPE-corrected and free energy values at $T = 10$ K are practically identical; however, higher temperatures slow down and disfavor the reactions as the energy barriers and the reaction energies increase slightly, by about 2 kcal mol^{-1} at the most. This is due to entropic effects since the computed relative enthalpy values differ only by 0.1–0.3 kcal mol^{-1} with respect to the ZPE-corrected ones. This is consistent with the facts that: (i) molecules in the TS need to be properly oriented in order to adopt a proton relay mechanism, so that the entropy decreases in the TS compared to the reactants; (ii) **P2-*ii*** (Fig. 3b) and **P3** (Fig. 4a) (products with one adsorbed molecule only) arise from the collision of two reactant molecules, so that their entropy is disfavored with respect to **R2-*ii*** and **R3**. Indeed, for cases in which the number of adsorbed species is the same in reactants and products (**P1**, Fig. 1 and **P4**, Fig. 4b) free energies almost coincide with ZPE-corrected profiles. Overall, these results indicate that an increase of temperature disfavors all the considered reactions due to unfavourable entropic contributions.

H_2O–ice bulk effects. The reactions shown above are meant to occur at the surface of H_2O–ice in which molecules from the gas-phase are adsorbed at the surface of icy grain particles. The considered model can, however, be confined within cavities of the icy mantles so that the reactive processes can suffer the effect of the dielectric response due to bulky ice. In quantum chemistry different strategies have been proposed to account for bulk effects, for instance when one needs to simulate solvent effects. In this respect, the continuum solvent field method is often employed due to its good balance between accuracy and simplicity.[77] This method, which has been also applied for biomolecular simulations,[78] represents the bulk as a continuous medium which is characterized by a dielectric constant, ε. Eyring and coworkers, in a seminal paper, reported the dielectric constant of various forms of ice, the value of ice Ih at 216.3 K being $\varepsilon = 114$.[79] Nevertheless, the actual value of the dielectric constant of the interstellar ices at cryogenic temperatures is vaguely known, so that in the present work the H_2O–ice cluster model including the adsorbates has been embedded in a continuum model with dielectric constant $\varepsilon = 78$, equal to that of liquid water.

Table 2 summarises the computed relative ZPE-corrected energies under the effect of bulk ice. Results indicate that bulk effects lower considerably some energy barriers, and especially those involving charged species. This is the case for Step 1 and Step 2-*ii*: in the former, the first energy barrier **TS1$_1$** decreases to 2 kcal mol^{-1} and the second **TS1$_2$** to 10 kcal mol^{-1}; in the latter, the overall energy profile lowers in energy due to the stabilization of the $(CN^-)/(NH_2{=}CH_2^+)$ ion pair, energy barriers being around 8–9 kcal mol^{-1}. Nonetheless, for the steps concerning the aminoacetonitrile hydrolysis (Step 3 and Step 4), although the barriers are lowered by some amount (specifically **TS4**, involving the zwitterion-like structure), they are still high (27–43 kcal mol^{-1}) to proceed at cryogenic temperatures.

Table 1 B3LYP/6-31+G(d,p) relative ZPE-corrected energy values ($\Delta_r U_0$) and relative Gibbs free energies ($\Delta_r G_T$) computed at different temperatures ($T = 10$, 100 and 200 K) of the stationary points involved in the most favorable paths of the glycine formation. Data in kcal mol^{-1}

Step 1	R1	$TS1_1$	$I1_1$	$I1_2$	$TS1_2$	P1
$\Delta_r U_0$	0.0	9.6	−7.1	−6.8	14.5	−6.2
$\Delta_r G_{10}$	0.0	9.6	−7.1	−6.8	14.6	−6.2
$\Delta_r G_{100}$	0.0	9.9	−6.9	−7.1	15.1	−6.2
$\Delta_r G_{200}$	0.0	10.8	−6.7	−7.5	16.2	−6.2
Step 2-*ii*	R2-*ii*	$TS2_1$-*ii*	I2-*ii*	$TS2_2$-*ii*	P2-*ii*	
$\Delta_r U_0$	0.0	17.5	15.5	16.2	−13.9	
$\Delta_r G_{10}$	0.0	17.8	15.7	16.4	−13.6	
$\Delta_r G_{100}$	0.0	18.6	16.7	17.1	−13.4	
$\Delta_r G_{200}$	0.0	20.1	18.2	18.2	−12.9	
Step 3	R3	$TS3_1$	I3	$TS3_2$	P3	
$\Delta_r U_0$	0.0	37.9	−3.5	4.8	−18.9	
$\Delta_r G_{10}$	0.0	39.2	−2.2	6.1	−16.7	
$\Delta_r G_{100}$	0.0	39.4	−2.1	6.8	−16.7	
$\Delta_r G_{200}$	0.0	40.2	−1.6	8.4	−16.4	
Step 4	R4	TS4	P4			
$\Delta_r U_0$	0.0	39.0	−3.0			
$\Delta_r G_{10}$	0.0	39.0	−3.0			
$\Delta_r G_{100}$	0.0	39.5	−2.7			
$\Delta_r G_{200}$	0.0	40.9	−2.4			

Table 2 B3LYP/6-31+G(d,p) relative ZPE-corrected energy values of the stationary points involved in the most favorable paths of the glycine formation for the isolated H_2O–ice cluster and when embedded in a water dielectric medium ($\varepsilon = 78$), [H_2O–ice]w, simulating the bulk ice. Data in kcal mol^{-1}

Step 1	R1	$TS1_1$	$I1_1$	$I1_2$	$TS1_2$	P1
H_2O–ice	0.0	9.6	−7.1	−6.8	14.5	−6.2
[H_2O–ice]w	0.0	1.9	−11.4	−11.3	9.6	−5.6
Step 2-*ii*	R2-*ii*	$TS2_1$-*ii*	I2-*ii*	$TS2_1$-*ii*	$P2_1$-*ii*	
H_2O–ice	0.0	17.5	15.5	16.2	−13.9	
[H_2O–ice]w	0.0	8.7	6.8	7.9	−19.8	
Step 3	R3	$TS3_1$	I3	$TS3_2$	P3	
H_2O–ice	0.0	37.9	−3.5	4.8	−18.9	
[H_2O–ice]w	0.0	33.9	−8.0	3.1	−21.8	
Step 4	R4	TS4	P4			
H_2O–ice	0.0	39.0	−3.0			
[H_2O–ice]w	0.0	29.6	−4.5			

Discussion and concluding remarks

Reactions between NH_3, $H_2C{=}O$ and HCN confined on or within interstellar and circumstellar H_2O–ice mantles have been investigated quantum mechanically at the B3LYP/6-31+G(d,p) level with the purpose of simulating the Strecker glycine synthesis in ICM. As a first step, the reaction mechanisms and the intrinsic role of water ice as catalyst have been studied. A water cluster (H_2O–ice model) extracted from the proton ordered crystalline ice phase XI, has been adopted to model the icy grain surface on which reactions have been computed.

Theoretical results show the relevance of the catalytic role of H_2O–ice by facilitating the proton transfers through a mechanism referred as "proton relay", in which water molecules belonging to rings of the icy surface behave simultaneously as proton acceptor/donor. The proton relay significantly lowers the energy barriers compared to gas-phase mechanisms, up to 30 kcal mol^{-1} as a maximum. Additionally, also some of the reaction energies are somehow more favorable in presence of H_2O–ice due to H-bonds with the ice surface. An important outcome of the present calculations has been to show that H_2O–ice surfaces strongly stabilize charged species, so that mechanisms involving ion pairs may become favoured. This is indeed the case for the reaction between HCN and $NH{=}CH_2$, in which the H_2O–ice surface stabilizes the $(CN^-)/(NH_2{=}CH_2^+)$ ion pair to be subsequently converted into aminoacteonitrile *via* almost barrierless direct C–C bond formation.

For reactions considered to occur on the surface of the ice water mantles theoretical calculations show that the first ($NH_3 + H_2C{=}O \rightarrow NH{=}CH_2 + H_2O$) and the second ($NH{=}CH_2 + HCN \rightarrow NH_2CH_2CN$) steps exhibit the lowest energy barriers, although still considerably high (between 10–18 kcal mol^{-1}) to occur at cryogenic temperatures. Hydrolysis of NH_2CH_2CN that finally yields glycine (here modeled by nucleophilic attack of two H_2O molecules) results in very high energy barriers. The computed reaction energies $\Delta_r U_0$ associated with different steps of the Strecker mechanism bringing reactants to glycine are in the −3 and −19 kcal mol^{-1} range, showing favorable thermodynamics.

Reactions considered to occur within ice cavities, where the long-range electrostatic effects exerted by the H_2O–ice bulk (here simulated by the inclusion of a dielectric continuum with $\varepsilon = 78$) are present, exhibit significantly lower energy barriers than those occurring at the H_2O–ice surface (see Table 2). For Step 1, such a lowering is indeed important in its first part *i.e.*, the NH_2CH_2OH formation, $\Delta U_0^{\neq}$ being reduced to 2 kcal mol^{-1}, but not enough as to reach the final $NH{=}CH_2$ product, as the computed $\Delta U_0^{\neq}$ from $\mathbf{I1_1}$ is 21 kcal mol^{-1}, too high for reactions at cryogenic temperatures. Accordingly, whereas the first part is expected to proceed the second one is hampered by kinetic reasons. These results are in full agreement with the experimental work of Bossa *et al.*,[25] in which the reaction between NH_3 and H_2CO to give NH_2CH_2OH was observed to occur in laboratory in the presence of interstellar ice analogs and by thermal activation, whereas the de-hydration step leading to $NH{=}CH_2$ was not observed. The kinetic barriers of Step 2 decrease to 8–9 kcal mol^{-1}, thus partly allowing the aminoacetonitrile formation in ICM conditions through charged intermediates. Calculations, however, show that glycine formation *via* aminoacetonitrile hydrolysis is hindered by too high kinetic barriers of the Step 3 and Step 4, namely $\Delta U_0^{\neq} = 34$ and 30 kcal mol^{-1}, respectively.

In summary, despite the dramatic energy barrier lowering caused by the action of H_2O–ice, some of the computed values are still exceedingly high, too high to allow the reactions to occur at cryogenic temperatures, and accordingly, suggest that glycine formation cannot proceed *via* Strecker-type mechanisms in its closed-shell formulation and *via* thermal promotion. Because of that, in addition to temperature, other substantial energy inputs available in space such as UV radiation or cosmic rays are required for the Strecker synthesis to be a reaction channel for glycine formation in ICM. Clearly, alternative mechanisms yielding glycine are also possible. For instance, the radical–radical mechanism studied by Woon[36] by means of highly accurate quantum-mechanical calculations, suggested glycine formation from a direct recombination of the COOH and NH_2CH_2 radicals which, in turn, were generated through several radical–radical complex reactions characterized by low energy barriers. A different proposal comes from the experimental work of Bossa *et al.*,[11] in which the formation of glycine in protostellar environments was simulated by studying the reaction of CO_2 and CH_3NH_2 in a water-dominated interstellar ice analog. In this work it was found that these two species thermally reacted to form the $[CH_3NH_3^+][CH_3NHCOO^-]$ salt, and, upon vacuum ultra-violet photolysis, this was converted to a glycine salt precursor $[CH_3NH_3^+][NH_2CH_2COO^-]$, whose presence is in line with the glycine and methylamine detection in the samples returned from the Stardust mission.

As quoted before, the barriers of aminoacetonitrile formation through Step 2 of the Strecker mechanism occurring within ice water cavities are of the order of 8–9 kcal mol^{-1}. These values, although slightly too high for cryogenic temperatures and in absence of UV, cannot exclude Step 2 as a possible channel towards aminoacetonitrile. The major concern to this channel, however, is the lack of $NH{=}CH_2$ reservoirs, due to the high energy barrier for its formation in the previous step.

Nonetheless $NH{=}CH_2$ can readily be achieved through other paths, as it is for instance the successive H addition to HCN ($HCN + 2H \rightarrow NH{=}CH_2$) predicted theoretically by Woon.[36] Accordingly, the present work predicts a possible channel for the aminoacetonitrile formation in the ICM, which arises from a combination of a radical–radical mechanism for $NH{=}CH_2$ formation and the Strecker-type $NH{=}CH_2$ + HCN reaction leading to NH_2CH_2CN. In that respect, new experimental measurements under highly controllable conditions, addressing the thermal reaction between $NH{=}CH_2$ and HCN would be welcome in order to validate whether Step 2 may occur at very low temperatures. In addition, calculations suggests that NH_2CH_2CN will not easily convert to glycine due to the high energy barriers, but will be accumulated, becoming part of the interstellar and circumstellar ice. This result seems to be consistent with the absence of the glcyine spectroscopic signature in ICM, at variance with that found for aminoacetonitrile.[18] Since nitriles are stable toward UV photolysis,[80] aminoacetonitrile could have been accumulated as a reservoir of glycine precursor in the interstellar ice mantles. It is then conceivable that aminoacetonitrile carried on cometary or interplanetary dust particles could have seeded the early Earth by micro-asteroidal bombardment, behaving as a potential source for glycine formation.

The present results will serve to plan new calculations in order to improve our understanding on chemical processes occurring at the ICM and in particular: (i) the ice water-mediated radical or excited state reactions of either the Strecker-type mechanism or other mechanisms such as that suggested by Bossa *et al.*,[11] thereby accounting for the effect of UV radiation on the processes; (ii) to account for isotopic effects on the reactions considered, as theoretical calculations are able to simulate the IR spectra of the species involved and to estimate the isotopic shifts to aid the detection of interstellar molecules and the elucidation of reaction paths.

Acknowledgements

A. R. is indebted to the Ramón Areces Foundation for a postdoctoral fellowship. Financial support from the Italian Ministry MIUR (Project COFIN2006, Prot. 2006032335_005) and from the Regione Piemonte (Bando ricerca scientifica Piemonte 2004, Settore: Nanotecnologie e nanoscienze, "Materiali nanostrutturati biocompatibili per applicazioni biomediche) is gratefully acknowledged. CESCA and CINECA supercomputing center is acknowledged for allowance of computer resources. Financial support from the Spanish MCYT (Project CTQ2008-06381) and Catalan DURSI (project 2009SGR-0638) are gratefully acknowledged. We thank the two anonymous reviewers for their helpful comments.

References

1 L. d'Hendecourt and E. Dartois, *Spectrochim. Acta, Part A*, 2001, **57**, 669–684.
2 E. F. v. Dishoeck, *Faraday Discuss.*, 1998, **109**, 31–46.
3 E. F. v. Dishoeck, *Annu. Rev. Astron. Astrophys.*, 2004, **42**, 119–167.
4 P. Ehrenfreund and S. B. Charnley, *Annu. Rev. Astron. Astrophys.*, 2000, **38**, 427–483.
5 D. C. B. Whittet, *Origins Life Evol. Biosphere*, 1997, **27**, 101–113.
6 D. E. Woon, Interstellar and circumstellar molecules (accessed 24 April 2009), http://www.astrochymist.org/astrochymist_ism.html.
7 P. Ehrenfreund and M. A. Sephton, *Faraday Discuss.*, 2006, **133**, 277–288.
8 S. Pizzarello, *Acc. Chem. Res.*, 2006, **39**, 231–237.
9 S. A. Sandford, J. Aléon, C. M. O. D. Alexander, T. Araki, S. Bajt, G. A. Baratta, J. Borg, J. P. Bradley, D. E. Brownlee, J. R. Brucato, M. J. Burchell, H. Busemann, A. Butterworth, S. J. Clemett, G. Cody, L. Colangeli, G. Cooper, L. D'Hendecourt, Z. Djouadi, J. P. Dworkin, G. Ferrini, H. Fleckenstein, G. J. Flynn, I. A. Franchi, M. Fries, M. K. Gilles, D. P. Glavin, M. Gounelle, F. Grossemy, C. Jacobsen, L. P. Keller, A. L. D. Kilcoyne, J. Leitner, G. Matrajt, A. Meibom, V. Mennella, S. Mostefaoui, L. R. Nittler, M. E. Palumbo, D. A. Papanastassiou, F. Robert, A. Rotundi, C. J. Snead, M. K. Spencer, F. J. Stadermann, A. Steele, T. Stephan, P. Tsou, T. Tyliszczak, A. J. Westphal, S. Wirick, B. Wopenka, H. Yabuta, R. N. Zare and M. E. Zolensky, *Science*, 2006, **314**, 1720–1724.
10 J. E. Elsila, D. P. Glavin and J. P. Dworkin, *Meteorit. Planet. Sci.*, 2009, **44**, 1323–1330.
11 J.-B. Bossa, F. Duvernay, P. Theulé, F. Borget, L. d'Hendecourt and T. Chiavassa, *Astron. Astrophys.*, 2009, **506**, 601–608.
12 Y.-J. Kuan, S. B. Charnley, H.-C. Huang, W.-L. Tseng and Z. Kisiel, *Astrophys. J.*, 2003, **593**, 848–867.
13 L. E. Snyder, *Origins Life Evol. Biosphere*, 1997, **27**, 115–133.
14 L. E. Snyder, F. J. Lovas, J. M. Hollis, D. N. Friedel, P. R. Jewell, A. Remijan, V. V. Ilyushin, E. A. Alekseev and S. F. Dyubko, *Astrophys. J.*, 2005, **619**, 914–930.
15 C. Ceccarelli, L. Loinard, A. Castets, A. Faure and B. Lefloch, *Astron. Astrophys.*, 2000, **362**, 1122–1126.
16 M. R. Cunningham, P. A. Jones, P. D. Godfrey, D. M. Cragg, I. Bains, M. G. Burton, P. Calisse, N. H. M. Crighton, S. J. Curran, T. M. Davis, J. T. Dempsey, B. Fulton, M. G. Hidas, T. Hill, L. Kedziora-Chudczer, V. Minier, M. B. Pracy, C. Purcell, J. Shobbrook and T. Travouillon, *Mon. Not. R. Astron. Soc.*, 2007, **376**, 1201–1210.
17 P. A. Jones, M. R. Cunningham, P. D. Godfrey and D. M. Cragg, *Mon. Not. R. Astron. Soc.*, 2007, **374**, 579–589.
18 A. Belloche, K. M. Menten, C. Comito, H. S. P. Müller, P. Schilke, J. Ott, S. Thorwirth and C. Hieret, *Astron. Astrophys.*, 2008, **482**, 179–196.
19 M. P. Bernstein, J. P. Dworkin, S. A. Sandford, G. W. Cooper and L. J. Allamandola, *Nature*, 2002, **416**, 401–403.
20 G. M. Muñoz-Caro, U. J. Meierhenrich, W. A. Schutte, B. Barbier, A. A. Segovia, H. Rosenbauer, W. H.-P. Thiemann, A. Brack and J. M. Greenberg, *Nature*, 2002, **416**, 403–406.
21 M. Nuevo, G. Auger, D. Blanot and L. d'Hendecourt, *Origins Life Evol. Biosphere*, 2008, **38**, 37–56.
22 Y. Takano, H. Masuda, T. Kaneko and K. Kobayashi, *Chem. Lett.*, 2002, **31**, 986–987.
23 P. Ehrenfreund, M. P. Bernstein, J. P. Dworkin, S. A. Sandford and L. J. Allamandola, *Astrophys. J.*, 2001, **550**, L95–L99.
24 W. A. Schutte, L. J. Allamandola and S. A. Sandford, *Science*, 1993, **259**, 1143–1145.
25 J.-B. Bossa, P. Theule, F. Duvernay and T. Chiavassa, *Astrophys. J.*, 2009, **707**, 1524–1532.
26 A. Strecker, *Ann. Chem. Pharm.*, 1850, **75**, 27–45.
27 A. Strecker, *Ann. Chem. Pharm*, 1854, **91**, 349–351.
28 S. L. Miller, *Science*, 1953, **117**, 528–529.
29 S. Miyakawa, H. Yamanashi, K. Kobayashi, H. J. Cleaves and S. L. Miller, *Proc. Natl. Acad. Sci. U. S. A.*, 2002, **99**, 14628–14631.
30 H. J. Cleaves, J. H. Chalmers, A. Lazcano, S. L. Miller and J. L. Bada, *Origins Life Evol. Biosphere*, 2008, **38**, 105–115.
31 H. Gröger, *Chem. Rev.*, 2003, **103**, 2795–2827.
32 J. E. Elsila, J. P. Dworkin, M. P. Bernstein, M. P. Martin and S. A. Sandford, *Astrophys. J.*, 2007, **660**, 911–918.
33 S. P. Walch, C. W. B. A. Ricca, Jr. and E. L. O. Bakes, *Chem. Phys. Lett.*, 2001, **333**, 6–11.
34 S. P. Walch and E. L. O. Bakes, *Chem. Phys. Lett.*, 2001, **346**, 267–273.
35 S. M. a. K. Ohno, *Astrophys. J.*, 2006, **640**, 823–828.

36 D. E. Woon, *Astrophys. J.*, 2002, **571**, L177–L180.
37 P. D. Holtom, C. J. Bennett, Y. Osamura, N. J. Mason and R. I. Kaiser, *Astrophys. J.*, 2005, **626**, 940–952.
38 N. Balucani, O. Asvany, A. H. H. Chang, S. H. Lin, Y. T. Lee, R. I. Kaiser, H. F. Bettinger, P. V. Schleyer and H. F. Schaefer, *J. Chem. Phys.*, 1999, **111**, 7472–7479.
39 N. Balucani, O. Asvany, A. H. H. Chang, S. H. Lin, Y. T. Lee and R. I. Kaiser, *J. Chem. Phys.*, 2000, **113**, 8643–8655.
40 L. C. L. Huang, O. Asvany, A. H. H. Chang, N. Balucani, S. H. Lin, Y. T. Lee and R. I. Kaiser, *J. Chem. Phys.*, 2000, **113**, 8656–8666.
41 D. M. Koch, C. l. Toubin, S. Xu, G. H. Peslherbe and J. T. Hynes, *J. Phys. Chem. C*, 2007, **111**, 15026–15033.
42 D. Courmier, F. Gardebien, C. Minot and A. St-Amant, *Chem. Phys. Lett.*, 2005, **405**, 357–363.
43 D. M. Koch, C. l. Toubin, G. H. Peslherbe and J. T. Hynes, *J. Phys. Chem. C*, 2008, **112**, 2972–2980.
44 D. E. Woon, *Icarus*, 1999, **142**, 550–556.
45 D. E. Woon, *Icarus*, 2001, **149**, 277–284.
46 D. E. Woon, *J. Phys. Chem. A*, 2001, **105**, 9478–9481.
47 D. E. Woon, *Int. J. Quantum Chem.*, 2002, **88**, 226–235.
48 J. P. D. Abbatt, *Chem. Rev.*, 2003, **103**, 4783–4800.
49 M. J. Frisch, G. W. Trucks, H. B. Schlegel, G. E. Scuseria, M. A. Robb, J. R. Cheesman, J. A. Montgomery, T. Vreven, K. N. Kudin, J. C. Burant, J. M. Millam, S. S. Iyengar, J. Tomasi, V. Barone, B. Mennucci, M. Cossi, G. Scalmanu, N. Rega, G. A. Petersson, H. Nakatsuji, M. Hada, M. Ehara, K. Toyota, R. Fukuda, J. Hasegawa, M. Ishida, T. Nakajima, Y. Honda, O. Kitao, H. Nakai, M. Klene, X. Li, J. E. Knox, H. P. Hratchian, J. B. Cross, C. Adamo, J. Jaramillo, R. Gomperts, R. E. Stratmann, O. Yazyev, A. J. Austin, R. Cammi, C. Pomelli, J. W. Ochterski, P. Y. Ayala, K. Morokuma, G. A. Voth, P. Salvador, J. J. Dannenberg, V. G. Zakrzewski, S. Dapprich, A. D. Daniels, M. C. Strain, O. Farkas, D. K. Malick, A. D. Rabuck, K. Raghavachari, J. B. Foresman, J. V. Ortiz, Q. Cui, A. G. Baboul, S. Clifford, J. Cioslowski, B. B. Stefanov, G. Liu, A. Liashenko, P. Piskorz, I. Komaromi, R. L. Martin, D. J. Fox, T. Keith, M. A. Al-Laham, C. Y. Peng, A. Nanayakkara, M. Challacombe, P. M. W. Gill, B. Johnson, W. Chen, M. W. Wong, C. Gonzalez and J. A. Pople, *GAUSSIAN 03*, Gaussian Inc., Wallingford CT, 2004.
50 A. D. Becke, *J. Chem. Phys.*, 1993, **98**, 5648–5652.
51 C. Lee, W. Yang and R. G. Parr, *Phys. Rev. B: Condens. Matter*, 1988, **37**, 785–789.
52 D. McQuarrie, *Statistical Mechanics*, Harper and Row, New York, 1986.
53 M. Cossi, N. Rega, G. Scalmani and V. Barone, *J. Comput. Chem.*, 2003, **24**, 669–681.
54 A. Klamt and G. Schueuermann, *J. Chem. Soc., Perkin Trans. 2*, 1993, 799–805.
55 J. M. Greenberg and A. Li, *Biol. Sci. Space*, 1998, **12**, 96–101.
56 H. M. Cuppen and E. Herbst, *Astrophys. J.*, 2007, **668**, 294–309.
57 M. E. Palumbo, *J. Phys. Conf. Ser.*, 2005, **6**, 211–216.
58 L. Hornekaer, A. Baurichter, V. V. Petrunin, A. C. Luntz, B. D. Kay and A. Al-Halabi, *J. Chem. Phys.*, 2005, **122**, 124701.
59 D. C. Jewitt and J. Luu, *Nature*, 2004, **432**, 731–733.
60 C. M. Lisse, J. VanCleve, A. C. Adams, M. F. A'Hearn, Y. R. Fernández, T. L. Farnham, L. Armus, C. J. Grillmair, J. Ingalls, M. J. S. Belton, O. Groussin, L. A. McFadden, K. J. Meech, P. H. Schultz, B. C. Clark, L. M. Feaga and J. M. Sunshine, *Science*, 2006, **313**, 635–640.
61 K. Malfait, C. Waelkens, J. Bouwman, A. D. Koter and L. B. F. M. Waters, *Astron. Astrophys.*, 1999, **345**, 181–186.
62 J. E. Chiar, *Origins Life Evol. Biosphere*, 1997, **27**, 79–100.
63 E. Lellouch, J. Crovisier, T. Lim, D. Bockelée-Morvan, K. Leech, M. S. Hanner, B. Altieri, B. Schmitt, F. Trotta and H. U. Keller, *Astron. Astrophys.*, 1998, **339**, L9–L12.
64 A. S. Bolina, A. J. Wolff and W. A. Brown, *J. Phys. Chem. B*, 2005, **109**, 16836–16845.
65 W. A. Brown, S. Viti, A. J. Wolff and A. S. Bolina, *Faraday Discuss.*, 2006, **133**, 113–124.
66 A. Allouche, P. Verlaque and J. Pourcin, *J. Phys. Chem. B*, 1998, **102**, 89–98.
67 J. D. Bernal and H. R. Fowler, *J. Chem. Phys.*, 1933, **1**, 515–548.
68 L. Pauling, *J. Am. Chem. Soc.*, 1935, **57**, 2680–2684.
69 T. Matsuoa, Y. Tajima and H. Suga, *J. Phys. Chem. Solids*, 1986, **47**, 165–173.
70 C. Pisani, S. Casassa and P. Ugliengo, *Chem. Phys. Lett.*, 1996, **253**, 201–208.
71 S. Casassa, P. Ugliengo and C. Pisani, *J. Chem. Phys.*, 1997, **106**, 8030–8040.
72 G. Bussolin, S. Casassa, C. Pisani and P. Ugliengo, *J. Chem. Phys.*, 1998, **108**, 9516–9528.
73 A. Erba, S. Casassa, L. Maschio and C. Pisani, *J. Phys. Chem. B*, 2009, **113**, 2347–2354.
74 J. W. Gauld, H. Audier, J. Fossey and L. Radom, *J. Am. Chem. Soc.*, 1996, **118**, 6299–6300.
75 J. W. Gauld and L. Radom, *J. Am. Chem. Soc.*, 1997, **119**, 9831–9839.
76 J.-Y. Park and D. E. Woon, *J. Phys. Chem. A*, 2004, **108**, 6589–6598.
77 J. Tomasi, B. Mennucci and R. Cammi, *Chem. Rev.*, 2005, **105**, 2999–3093.
78 M. S. Lee, F. R. S. Jr. and M. A. Olson, *J. Comput. Chem.*, 2004, **25**, 1967–1978.
79 M. E. Hobbs, M. S. Jhon and H. Eyring, *Proc. Natl. Acad. Sci. U. S. A.*, 1966, **56**, 31–38.
80 M. P. Bernstein, S. F. M. Ashbourn, S. A. Sandford and L. J. Allamandola, *Astrophys. J.*, 2004, **601**, 365–370.

